Polymorphism, isostructurality and variability in the inclusion chemistry of a diol host compound†

Luigi R. Nassimbeni,*[a] Hong Su[a] and Edwin Weber[b]

Received (in Montpellier, France) 8th February 2008, Accepted 21st April 2008
First published as an Advance Article on the web 4th July 2008
DOI: 10.1039/b802269k

The diol host compound 2,2′-bis(hydroxydiphenylmethyl)-1,1′-binaphthyl crystallised in three different polymorphic structures, and formed a series of inclusion compounds with pyridine, morpholine and benzene. Different stoichiometries were obtained by manipulating the proportions of the guests and the crystallisation temperatures. A number of these compounds are isostructural and the guests are located at fixed sites in the crystal structure. Structural similarities were interpreted *via* Hirshfeld surface fingerprint plots. The results of thermal analysis of one structural group were explained in terms of the host···guest interactions.

Introduction

The process of molecular recognition in inclusion compounds is governed by the intermolecular interactions which occur between the various host and guest molecules making up the resultant crystalline assembly. The synthesis of a successful host is guided by certain principles, enunciated by Weber,[1] who has shown that the molecule should be bulky and rigid and preferably contain functional groups which can engage in specific host–guest interactions. We have studied a number of bulky diol host compounds which form inclusion compounds with a variety of guests. Their structures have been correlated with their thermal stabilities, their kinetics of desorption and enclathration and the selectivity they exhibit towards a particular guest when exposed to a guest mixture.[2–4] Weber has reviewed the concepts of shape and symmetry in the design of efficient host compounds,[5] of which one of the most successful is the 'wheel-and-axle' or 'dumbbell' sort. These contain a long linear axis and bulky substituents at both ends, of which the aristotype is the compound 1,1,6,6-tetraphenylhexa-2,4-diyne-1,6-diol. This host has been studied extensively.[6–8] The wheel and axle concept has been extended by Bacchi *et al.*,[9,10] who incorporated metals into the spacers. Bacchi *et al.* proposed a molecular mechanism, likened to the workings of 'Venetian blinds', in order to explain the process of solvation and desolvation which occurs when these compounds react with volatile guests. Another important category of host compounds is that based on the 'scissors' design, in which the motif has twofold symmetry (C_2). Good examples are 1,1′-binaphthyl-2,2′-dicarboxylic acid and 2,2′-dihydroxy-1,1′-binaphthyl (binaphthol).[11]

In this work we consider the related host 2,2′-bis(hydroxydiphenylmethyl)-1,1′-binaphthyl (**H**), the structure of which, both in the form of the apohost, $\mathbf{H_1}$, and as the host in the inclusion compound with pyridine, **H·3P**, has been previously studied.[12] We present the structures of two further polymorphs of the apohost, $\mathbf{H_2}$ and $\mathbf{H_3}$, as well as those of the inclusion compounds with various combinations of pyridine (**P**), morpholine (**M**) and benzene (**B**). The numbering scheme of the host and guests are shown in Scheme 1.

Results and discussion

Crystal structures

The crystallographic data for the three polymorphs of the apohost, $\mathbf{H_1}$, $\mathbf{H_2}$ and $\mathbf{H_3}$ and for the four iso-structural compounds **H·3P**, **H·2P·M**, **H·2P·B** and **H·P·M·B** are given in Table 1, and those for **H·M**, **H·3M**, **H·2P·3M**, **H·2M·0.5B** and **H·M·1.5B** are given in Table 2.

The structure of $\mathbf{H_1}$ and **H·3P** have been published previously[12] but their crystal data is repeated to allow ready comparison with the other structures.

The conformation of the host molecule, in all the structures, is remarkably constant. Steric considerations require the two naphthyl moieties, with bulky groups at the 2,2′-positions, to lie approximately perpendicular to each other. The hydroxyl

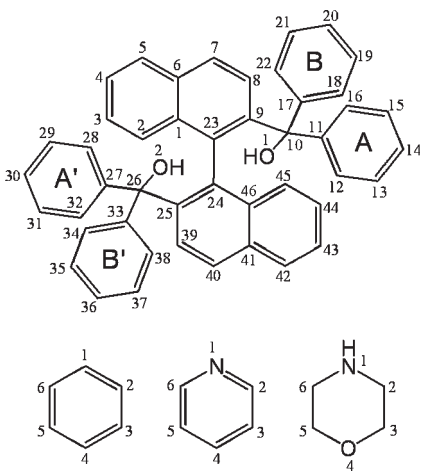

Scheme 1 Atomic nomenclature.

[a] *Department of Chemistry, University of Cape Town, Rondebosch, 7701 Cape Town, South Africa. E-mail: luigi.nassimbeni@uct.ac.za; Fax: +27-21-685 4580; Tel: +27-21-6502569*
[b] *Institut für Organische Chemie, Technische Universität, Bergakademie Freiberg, Leipziger Strasse 29, D-09596 Freiberg/Sachsen, Germany. E-mail: Edwin.Weber@chemie.tu-freiberg.de*

† CCDC reference number 685680. For crystallographic data in CIF or other electronic format see DOI: 10.1039/b802269k

Table 1 X-Ray data and refinement parameters for the three polymorphs (**H_1**, **H_2** and **H_3**) and structures **H·3P**, **H·2P·M**, **H·2P·B** and **H·P·M·B**

	H_1[a]	**H_2**	**H_3**	**H·3P**[a]	**H·2P·M**	**H·2P·B**	**H·P·M·B**
Structure formula	$C_{46}H_{34}O_2$	$C_{46}H_{34}O_2$	$C_{46}H_{34}O_2$	$C_{46}H_{34}O_2 \cdot 3C_5H_5N$	$C_{46}H_{34}O_2 \cdot 2C_5H_5N \cdot C_4H_9NO$	$C_{46}H_{34}O_2 \cdot 2C_5H_5N \cdot C_6H_6$	$C_{46}H_{34}O_2 \cdot C_5H_5N \cdot C_4H_9NO \cdot C_6H_6$
M_r	618.73	618.73	618.73	856.08	864.10	855.04	863.06
T/K	293(2)	113(2)	113(2)	293(2)	113(2)	113(2)	113(2)
Crystal symmetry	Orthorhombic	Monoclinic	Monoclinic	Triclinic	Triclinic	Triclinic	Triclinic
Space group	$P2_12_12_1$	$P2_1/n$	$Pna2_1$	$P\bar{1}$	$P\bar{1}$	$P\bar{1}$	$P\bar{1}$
a/Å	8.080(1)	8.3281(1)	22.2928(6)	12.541(3)	12.4246(3)	12.4021(2)	12.395(2)
b/Å	16.709(4)	35.9201(5)	17.9763(4)	12.643(5)	12.5638(3)	12.5903(2)	12.491(2)
c/Å	24.032(5)	10.8520(2)	8.0147(2)	15.684(2)	15.4671(3)	15.4556(3)	15.500(3)
α/°	90	90	90	82.78(2)	82.825(1)	82.465(1)	82.46(1)
β/°	90	105.819(1)	90	76.05(1)	76.239(1)	76.078(1)	75.89(1)
γ/°	90	90	90	82.76(2)	81.880(1)	81.878(1)	81.42(1)
V/Å^3	3245(1)	3123.39(8)	3211.8(1)	2382(1)	2311.1(2)	2307.06(4)	2290.1(7)
Z	4	4	4	2	2	2	2
D_c/g cm^{-3}	1.27	1.316	1.280	1.19	1.242	1.231	1.252
μ/mm^{-1}		0.079	0.077		0.076	0.074	0.076
F(000)		1304	1304		916	904	916
Crystal size/mm		0.07 × 0.10 × 0.11	0.04 × 0.08 × 0.13		0.10 × 0.15 × 0.20	0.33 × 0.40 × 0.42	0.10 × 0.12 × 0.14
2θ range/°		2.81–25.33	2.27–25.36		2.74–25.34	3.33–25.35	2.41–25.52
Limiting indices		±10; ±43; ±13	±26; ±21; ±9		±14; ±15; ±18	±14; ±15; ±18	±14; ±15; ±18
Reflections collected/unique		11 181/5663	5690/3159		8373/5330	16 134/8382	13 871/7667
No. parameters/ restraints		442/2	440/3		604/3	604/2	568/4
Extinction coefficient		0.0027(5)	0.0080(8)		0.0081(1)	0.009(1)	
Goodness-of-fit on F^2		0.923	0.964		1.021	1.051	1.017
Final R indices [$I > 2\sigma(I)$]		$R1$ = 0.0395 $wR2$ = 0.0767	$R1$ = 0.0376 $wR2$ = 0.0726		$R1$ = 0.0470 $wR2$ = 0.1135	$R1$ = 0.0380 $wR2$ = 0.0958	$R1$ = 0.1036 $wR2$ = 0.2694
R indices (all data)		$R1$ = 0.0849 $wR2$ = 0.0889	$R1$ = 0.0637 $wR2$ = 0.0812		$R1$ = 0.0914 $wR2$ = 0.1320	$R1$ = 0.0482 $wR2$ = 0.1041	$R1$ = 0.1600 $wR2$ = 0.3219
$\Delta\rho_{max,\ min}$/e Å^{-3}		0.190/−0.195	0.194/−0.188		0.476/−0.318	0.224/−0.368	1.384/−0.972

[a] Cell dimensions are from ref. 12.

groups are thus forced into proximity, resulting in an intramolecular hydrogen bond O1–H1···O2, a constant feature in all the structures. The conformation of the host is governed by the seven torsion angles τ_1–τ_7, listed for all structures in Table 3. The details of hydrogen bonding for all structures are in Table 4. The conformation of the host molecule is such that two of the phenyl rings A and A′ lie in close proximity to the naphthyl moieties and the other two rings, B and B′, point away from the central bond C23–C24. τ_1, the torsion angle about the central C23–C24 bond, varies over a narrow range from 94.2(2)° to 98.6(6)°. The variation in the torsion angles τ_2–τ_7 is more pronounced in the apohost structures **H_1**, **H_2** and **H_3** than in the clathrates, a possible reasons for the host polymorphism. This is illustrated in Fig. 1, which shows a molecule of host from the structure **H_3** viewed along the central bond C23–C24, which displays the O1–H1···O2 hydrogen bond as well as the dispositions of the four phenyl rings and the seven torsion angles.

The second polymorph, **H_2**, crystallised in the space group $P2_1/n$ with Z = 4, while the third polymorph, **H_3**, crystallised in the space group $Pna2_1$ with Z = 4. Projections of the three polymorphs are displayed in Fig. 2 together with their Hirshfeld surface fingerprint plots.[14,15] The powder X-ray diffraction patterns calculated from the crystallographic data for **H_1**, **H_2** and **H_3** are shown in Fig. 3. We have computed the Hirshfeld surfaces of the three polymorphs using the CrystalExplorer program.[16] For **H_1**, the spike labelled 1 in Fig. 2 with $d_e = d_i \cong 1.08$ Å is due to intermolecular H···H contacts, and this features is weaker in the plots for **H_2** and **H_3**. Polymorph **H_1** also exhibits two distinct spikes (labelled 2) associated with C···H contacts which also occur in maps for **H_2** and **H_3**. From these fingerprints we can derive the areas associated with H···H, C···H and O···H contacts which yield the following:

H_1	71%	26%	2%
H_2	67%	30%	2%
H_3	69%	29%	2%

This emphasises the predominance of H···H contacts.

The inclusion compounds **H·3P**, **H·2P·M**, **H·2P·B** and **H·P·M·B** are isostructural, all crystallising in the space group $P\bar{1}$ with Z = 2 and similar cell dimensions. The locations of the three sites occupied by the guests are the same irrespective of the nature of the guest. This is illustrated schematically in

Table 2 X-ray data and refinement parameters for **H·M**, **H·3M**, **H·2P·3M**, **H·2M·0.5B** and **H·M·1.5B**

	H·M	**H·3M**	**H·2P·3M**	**H·2M·0.5B**	**H·M·1.5B**
Structure formula	$C_{46}H_{34}O_2{\cdot}C_4H_9NO$	$C_{46}H_{34}O_2{\cdot}3C_4H_9NO$	$C_{46}H_{34}O_2{\cdot}3C_4H_9NO{\cdot}2C_5H_5N$	$C_{46}H_{34}O_2{\cdot}2C_4H_9NO{\cdot}0.5C_6H_6$	$C_{46}H_{34}O_2{\cdot}C_4H_9NO{\cdot}1.5C_6H_6$
M_r	705.05	880.10	1038.3	832.03	823.02
T/K	113(2)	113(2)	113(2)	113(2)	113(2)
Crystal symmetry	Orthorhombic	Triclinic	Triclinic	Monoclinic	Monoclinic
Space group	*Pbca*	$P\bar{1}$	$P\bar{1}$	$P2_1/n$	$P2_1/n$
a/Å	20.6273(2)	11.559(1)	12.4117(4)	12.7375(2)	12.7331(2)
b/Å	16.9073(2)	11.522(1)	13.4626(5)	34.2660(5)	33.9999(5)
c/Å	21.0569(3)	18.781(2)	17.8740(6)	20.5820(3)	20.7113(3)
α/°	90	74.075(2)	96.424(1)	90	90
β/°	90	98.348(3)	90.779(1)	94.948(1)	95.175(1)
γ/°	90	90.650(3)	106.662(1)	90	90
V/Å^3	7343.6(2)	2378.8(4)	2839.99(2)	8949.8(2)	8929.9(2)
Z	8	2	2	8	8
D_c/g cm^{-3}	1.277	1.229	1.214	1.235	1.224
μ/mm^{-1}	0.078	0.078	0.077	0.077	0.074
$F(000)$	2992	940	1108	3544	3496
Crystal size/mm	0.07 × 0.12 × 0.15	0.10 × 0.14 × 0.16	0.16 × 0.18 × 0.22	0.18 × 0.23 × 0.30	0.15 × 0.22 × 0.25
2θ range/°	3.29–25.36	2.42–25.00	2.63–25.33	1.96–24.69	3.00–25.33
Limiting indices	±24; ±20; ±25	±13; ±13; ±22	±14; ±16; ±21	±14; 35,40; ±24	±15; ±40; ±24
Reflections collected/unique	12 779/6699	15 009/8315	19 693/10 266	27 807/15 040	29 167/15 922
No. parameters/restraints	498/3	497/2	605/2	1074/5	1151/6
Extinction coefficient	0.0019(5)	0.0064(4)		0.0050(9)	0.0006(2)
Goodness-of-fit on F^2	1.046	1.330	1.481	1.019	1.049
Final R indices	$R1$ = 0.0545	$R1$ = 0.1497	$R1$ = 0.1325	$R1$ = 0.1097	$R1$ = 0.0783
[$I > 2\sigma(I)$]	$wR2$ = 0.1524	$wR2$ = 3964	$wR2$ = 0.3776	$wR2$ = 0.2923	$wR2$ = 0.2005
R indices (all data)	$R1$ = 0.0895	$R1$ = 0.2522	$R1$ = 0.1994	$R1$ = 0.1589	$R1$ = 0.1624
	$wR2$ = 0.1716	$wR2$ = 0.4526	$wR2$ = 0.4240	$wR2$ = 0.3307	$wR2$ = 0.2398
$\Delta\rho_{max,\ min}$/e Å^{-3}	0.609/−0.379	1.322/−0.840	1.586/−1.212	1.400/−0.794	1.023/−0.671

Table 3 Torsion angles of the host molecule occurred in all structures

	τ_1	τ_2	τ_3	τ_4	τ_5	τ_6	τ_7
H$_1$[a]	95(1)	−31(1)	59(1)	47.7(9)	−48.4(9)	51.4(9)	59.1(9)
H$_2$	94.2(2)	−18.8(2)	77.6(2)	26.0(2)	−42.5(2)	54.8(2)	53.1(2)
H$_3$	95.0(3)	−36.4(3)	39.5(3)	75.2(3)	−46.4(3)	56.1(3)	55.4(3)
H·3P[a]	97(2)	−31(1)	41(2)	57.1(9)	−44.2(8)	57.2(9)	63.1(9)
H·2P·M	95.7(2)	−31.1(2)	40.3(2)	56.2(2)	−44.9(2)	58.3(2)	64.4(2)
H·2P·B	95.8(2)	−30.6(2)	38.8(2)	56.4(1)	−45.0(1)	58.5(1)	64.9(1)
H·P·M·B	95.7(6)	−30.6(6)	41.6(6)	56.7(5)	−45.1(6)	58.1(5)	64.5(5)
H·M	97.6(3)	−33.0(3)	59.9(3)	52.2(3)	−38.0(3)	57.4(3)	58.0(3)
H·3M	98.3(8)	−37.2(8)	50.8(8)	59.3(9)	−41.9(9)	55.9(8)	57.6(8)
H·2P·3M	98.6(6)	−34.4(6)	52.2(6)	58.1(6)	−39.6(6)	56.3(6)	60.5(6)
H·2M·0.5B	95.2(6)	−39.4(6)	59.6(6)	52.4(6)	−35.6(6)	57.4(6)	54.0(6)
	95.2(6)	−37.0(5)	62.2(5)	56.0(5)	−40.2(6)	54.6(6)	60.8(6)
H·M·1.5B	95.3(4)	−37.6(5)	59.0(4)	52.7(4)	−35.9(5)	56.5(4)	52.6(5)
	96.2(5)	−36.1(4)	62.5(4)	55.8(4)	−39.0(5)	55.3(4)	60.8(5)

[a] The torsion angles for **H$_1$** and **H·3P** are computed using program PLATON[13] from their CIF files extracted from CSD (refcode WAPBUK and WAPCAR, respectively).

Fig. 4. Site I ($x \cong 0.17$, $y \cong -0.07$, $z \cong 0.23$) is always taken by a pyridine molecule and displays a hydrogen bond: (host)-O–H···N(pyridine) with O···N in the range 2.735(5)–2.78(1) Å in all four structures. In **H·3P** the other two pyridines are at site II ($x \cong 0.69$, $y \cong -0.06$, $z \cong 0.25$) and site III ($x \cong 0.02$, $y \cong 0.24$, $z \cong 0.02$) and are not hydrogen bonded. In the **H·2P·M** structure, the morpholine located at site II is also hydrogen bonded *via* a (morpholine)N–H···O(host) bond with d(N···O) = 3.119(2) Å. The **H·2P·B** structure simply replaces a pyridine with benzene at site III and **H·P·M·B** is similar to **H·2P·M** in that both the pyridine and the morpholine are engaged in hydrogen bonding and benzene is located in site III. The packing of the structure **H·P·M·B**, which is representative of all four structures in this group, is shown in Fig. 5. The Hirshfeld surface fingerprint plots for these four structures are shown in Fig. 6. In each case the surfaces only envelop the host molecule. For **H·3P**, the spike labelled 1 is associated with the (host)O–H···N(pyridine) hydrogen bond. This plot is similar for **H·2P·B**. The plot for **H·2P·M** has an additional spike labelled 2 which corresponds to (morpholine)-N–H···O(Host) hydrogen bond. This feature was expected for **H·P·M·B** but does not occur, probably due to the inaccurate position of the amino hydrogen. In the **H·P·M·B** structure, the morpholine exhibits high atomic temperature factors and

Table 4 Hydrogen bonding details (d/Å, ∠/°) for all structures (D = donor, A = acceptor)

	d(D–H)	d(H···A)	d(D···A)	∠(D–H···A)
H_1[a]				
O1–H1···O2	0.97(3)	1.81(3)	2.759(7)	167(6)
H_2				
O1–H1···O2	0.98(2)	2.05(2)	2.951(2)	152(2)
H_3				
O1–H1···O2	0.98(1)	1.82(1)	2.780(3)	170(2)
H·3P[a]				
O1–H1···O2	1.03(3)	1.65(3)	2.68(1)	175(3)
O2–H2···N1G	0.97(2)	1.81(3)	2.78(1)	174(3)
H·2P·M				
O1–H1···O2	0.97(2)	1.70(2)	2.660(2)	169(2)
O2–H2···N1A	0.98(2)	1.77(2)	2.743(2)	174(2)
N1B–H1B···O1	0.99(2)	2.22(3)	3.119(2)	150(2)
H·2P·B				
O1–H1···O2	0.97(1)	1.71(2)	2.670(1)	172(2)
O2–H2···N1A	0.98(2)	1.77(2)	2.748(1)	173(2)
H·P·M·B				
O1–H1···O2	1.00(2)	1.67(2)	2.660(4)	172(7)
O2–H2···N1A	0.99(2)	1.75(2)	2.735(5)	173(6)
N1B–H1B···O1	0.92	2.79	3.165(8)	105.7
H·M				
O1–H1···O2	0.98(2)	1.75(2)	2.700(2)	162(3)
O2–H2···N1G	1.00(2)	1.84(2)	2.823(3)	169(3)
H·3M				
O1–H1···O2	0.97(2)	1.76(3)	2.695(7)	162(6)
O2–H2···N1A	0.98(2)	1.79(4)	2.71(2)	153(6)
H·2P·3M				
O1–H1···O2	0.99(2)	1.65(2)	2.635(5)	174(5)
O2–H2···N1A	0.99(2)	1.73(2)	2.724(6)	175(5)
H·2M·0.5B				
O1X–H1X···O2X	1.00(2)	1.74(3)	2.717(4)	164(5)
O2X–H2X···N1A	1.00(2)	1.73(2)	2.728(5)	178(5)
O1Y–H1Y···O2Y	0.99(2)	1.71(3)	2.674(4)	165(7)
O2Y–H2Y···N1B	1.01(2)	1.77(3)	2.750(6)	163(5)
H·M·1.5B				
O1X–H1X···O2X	0.99(2)	1.75(2)	2.721(4)	168(5)
O2X–H2X···N1A	1.00(2)	1.73(2)	2.727(4)	171(4)
O1Y–H1Y···O2Y	1.00(2)	1.69(2)	2.670(3)	165(4)
O2Y–H2Y···N1B	1.00(2)	1.77(2)	2.750(4)	167(4)

[a] The H-bond matrices are from ref. 12.

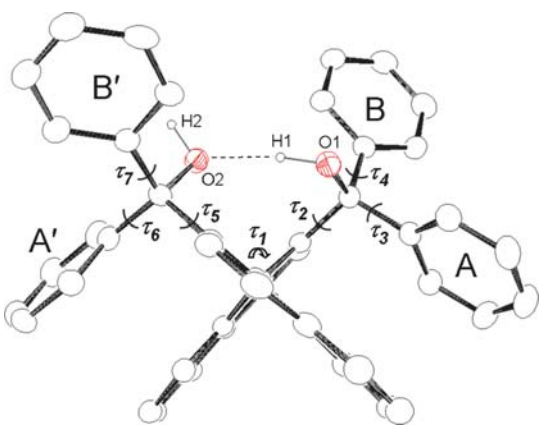

Fig. 1 Host molecular structure from the polymorph H_3, showing the intramolecular O–H···O hydrogen bond and the torsion angles.

the hydrogens could not be located on the final difference electron density map. We therefore placed the hydrogens in geometrically idealised positions, choosing the equatorial conformation for the amino hydrogen.

H·M crystallised in the space group *Pbca* with $Z = 8$. The important feature is the (host)O–H···N(morpholine) hydrogen bond with d(O···N) = 2.823(3) Å, as shown in Fig. 7. The morpholine is located in cavities, rendering this structure very stable, a fact that we observed when handling the crystals.

The crystal of **H·3M** was unstable and several data collection were carried out before we would obtain a suitable intensity data set. The final refinement was not wholly satisfactory and the atoms of the morpholine guests could only be refined with isotropic temperature factors, some of which had high values. One of the morpholine guests is hydrogen bonded *via* (host)O–H···N(morpholine) with d(O···N) = 2.72(2) Å. Projections of the structure, showing only the host molecules in van der Waals representation, display crossing channels in which the guest molecules are located, and are shown in Fig. 8.

Problems were also encountered with the structure solution of **H·2P·3M**, in that the crystals obtained were highly unstable. All three morpholine molecules could only be refined with isotropic temperature factors and their H atoms were not located and were left out of the final model. A projection of the structure, viewed along [100], is shown in Fig. 9, and is characterised by alternating layers of host and mixed guest layers, resulting in an open framework, which explain the instability of this compound.

The final two structures, **H·2M·0.5B** and **H·M·1.5B**, are isostructural with similar cell parameters and crystallised in the space group $P2_1/n$ with $Z = 8$. Thus in **H·2M·0.5B**, there are two crystallographically independent host molecules, one benzene and three morpholines in general positions and the remaining morpholine is located at two different centres of inversion, at Wyckoff positions a and b. Symmetry requires these morpholines to be disordered, so that they were modelled with coincident O and N atoms with site occupancies of 0.5. One morpholine guest is H-bonded to each host *via* (host)O–H···N(morpholine) with O···N distances of 2.728(5) and 2.750(6) Å, respectively.

The structure of **H·M·1.5B** is similar, but in this case one benzene is located on two different centres of inversion. One of the morpholines is disordered and was successfully modelled. Both morpholines are H-bonded as in the previous structure.

The packing, shown in Fig. 10, is characterised by channels which run parallel to [100], in which the guest molecules are located.

The conformational feature of this host, with the two naphthyl moieties at right angle and locked by an intramolecular hydrogen bond, is repeated in similar hosts.

Thus in the analogous compound 2,2′-bis(hydroxydiphenylmethyl)-1,1′-biphenyl which forms inclusion compounds with benzene and water,[17] the central torsion angle in the biphenyl is twisted to 100° and is stabilised by an intramolecular O–H···O hydrogen bond. The related host 2,2′-bis(9-hydroxy-9-fluorenyl)biphenyl and its inclusion compounds with acetonitrile, cyclohexanone, di-*n*-propylamine and dimethylformamide has also been studied.[18] In each case the two biphenyl rings are perpendicular and fixed by an intramolecular O–H···O hydrogen bond. This latter host is atropisomeric and was resolved by recrystallisation with (−)-fenchone with which it forms an inclusion compound with host : guest stoichiometry of 1 : 2. The recovered optically pure host is enantioselective and has been employed in the

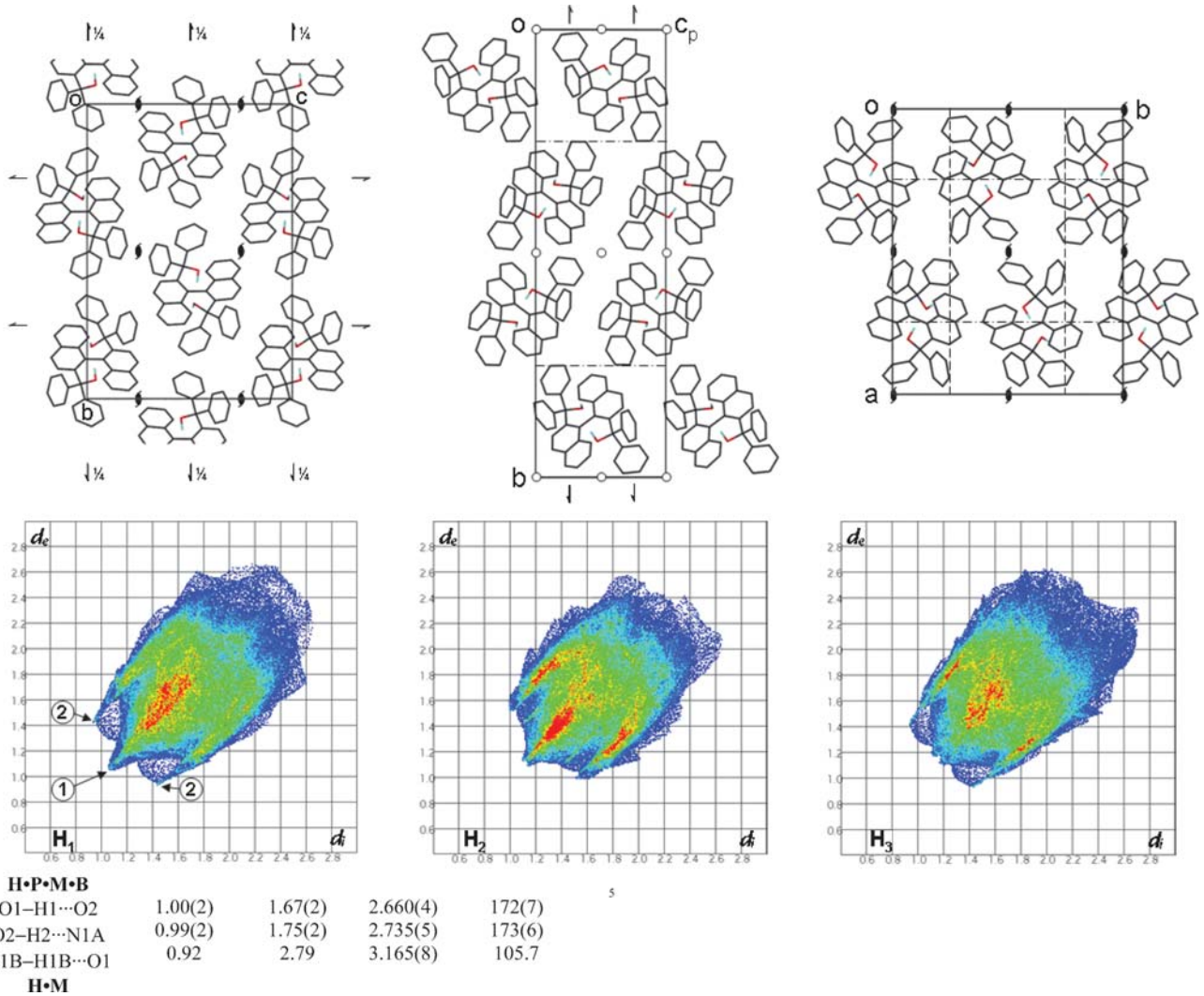

Fig. 2 Projections and Hirshfeld surface fingerprint plots of the polymorphs $\mathbf{H_1}$, $\mathbf{H_2}$ and $\mathbf{H_3}$.

resolution of racemates.[19] Recent studies of this host were directed at the formation of infinitely connected networks by the synthesis of inclusion compounds with multifunctional guest molecules, namely diethylene glycol, bis(2-aminoethyl)-amine, methacrylic acid and 2-cyclopenten-1-one. However they formed discrete 2 : 2 host–guest aggregates and conventional host–guest units, testifying to the stability of the host conformation characterised by the perpendicular biphenyl rings and the concomitant intramolecular hydrogen bond.[20]

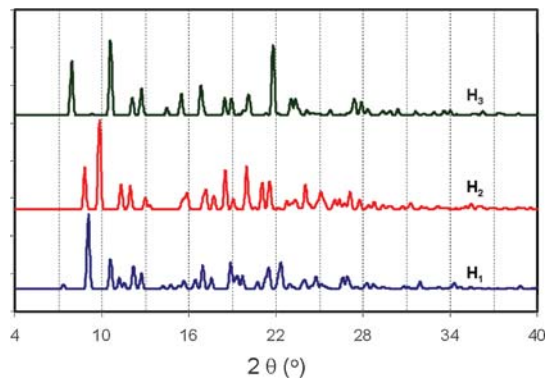

Fig. 3 Calculated X-ray powder diffraction patterns for $\mathbf{H_1}$, $\mathbf{H_2}$ and $\mathbf{H_3}$.

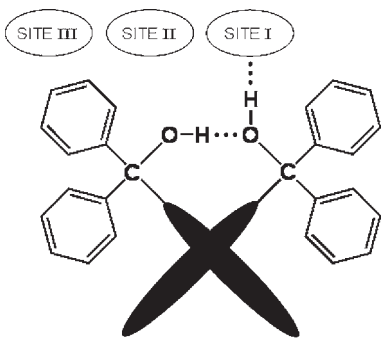

Structure codes	SITE I	SITE II	SITE III
H•3P	P	P	P
H•2P•M	P	M	P
H•2P•B	P	P	B
H•P•M•B	P	M	B

Fig. 4 Schematic diagram of the host molecule and the three guest sites.

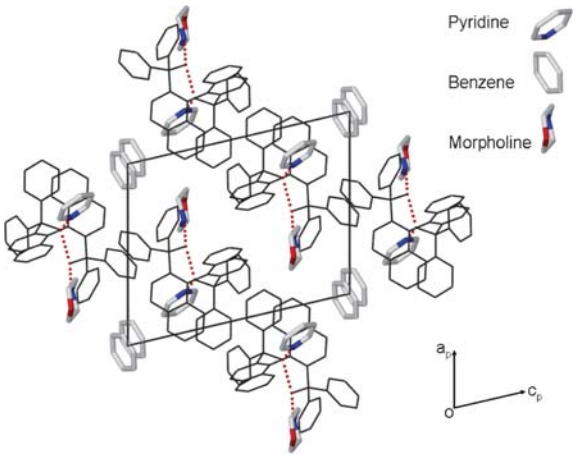

Fig. 5 Projection viewed along [010] of **H·P·M·B**.

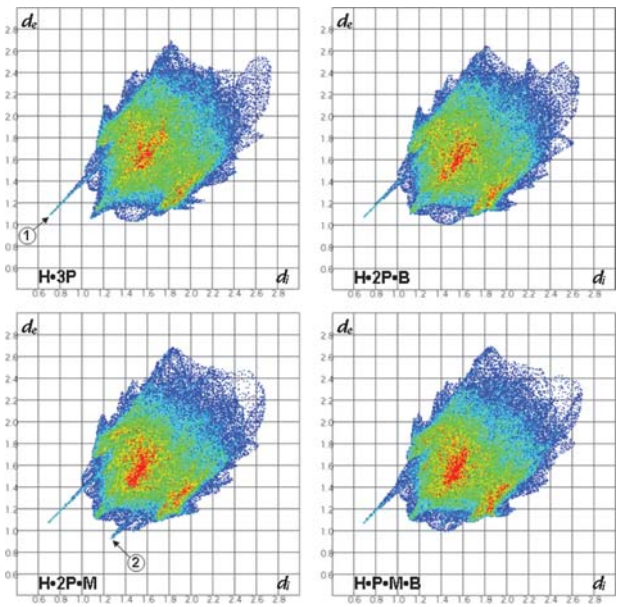

Fig. 6 Hirshfeld fingerprints for **H·3P**, **H·2P·M**, **H·2P·B** and **H·P·M·B**.

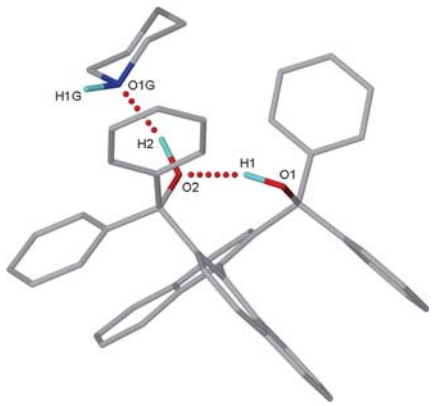

Fig. 7 Molecular structure of **H·M**, showing the hydrogen bonds and the amino hydrogen in the equatorial position.

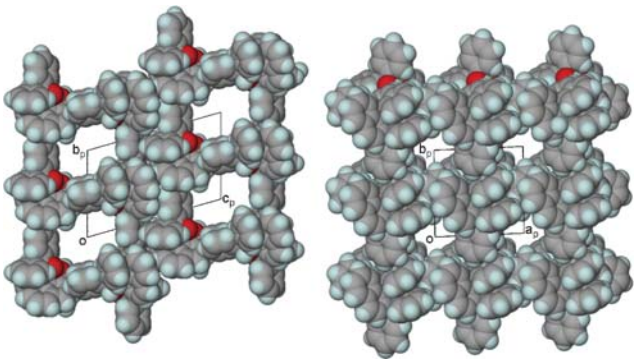

Fig. 8 Projections viewed along [100] and [001] for **H·3M**, showing the location of the open channels. All guest molecules are omitted.

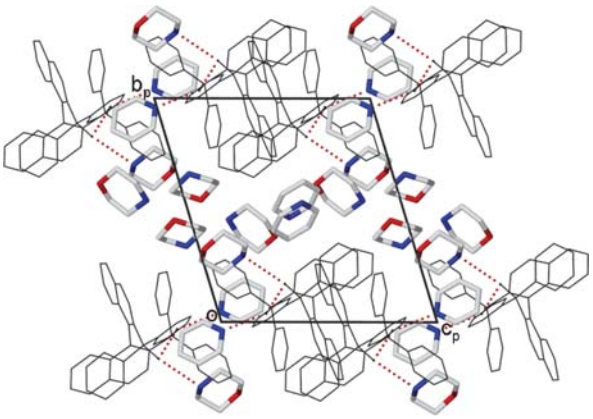

Fig. 9 Layered structure of **H·2P·3M** viewed along [100].

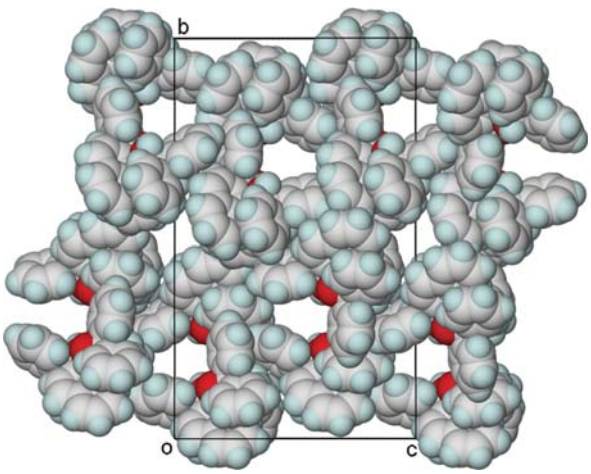

Fig. 10 Channel structure of **H·M·1.5B** viewed along [100]. All guest molecules are omitted.

Thermal analysis

The results of the thermal analysis for **H·2P·M**, **H·2P·B** and **H·P·M·B** are shown in Fig. 11 and in Table 5. The TG curves are similar to those obtained for the **H·3P** compound[12] in that the guest loss occurs in two steps and we interpret the first step to be for the guest molecules which are located at site II and III, and the second step for the loss of the H-bonded pyridine, located at site I.

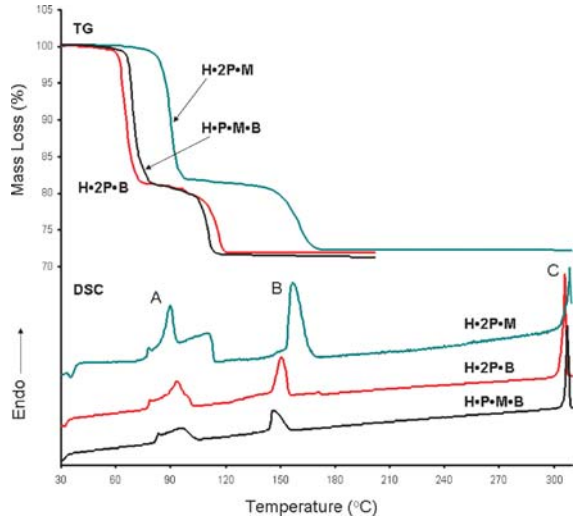

Fig. 11 TG and DSC curves of **H·2P·M**, **H·2P·B** and **H·P·M·B**.

Table 5 TG results [found (calc.) wt%] for **H·2P·M**, **H·2P·B** and **H·P·M·B**

Compound	1st step	2nd step
H·2P·M	18.2 (19.2)	27.8 (28.4)
H·2P·B	18.8 (18.4)	28.0 (27.6)
H·P·M·B	18.8 (19.1)	28.2 (28.3)

We note that the TG curves for **H·2P·M** is displaced to significantly higher temperatures. We interpret this by noting that the normal boiling point of benzene (80.1 °C) is considerably lower than that of pyridine (115.6 °C) or morpholine (128.0 °C). Therefore for **H·2P·B** and **H·P·M·B** benzene is released at lower temperatures (~65 °C), causing the crystallites to crumble to a fine powder with increased surface area, easing the subsequent release of the pyridine. The corresponding DSC curves all show three endotherms: A, a complex endotherm corresponding to the loss of the first two guests; B, the second endotherm assigned to the H-bonded pyridine and C, the endotherm due to the host melt. We obtained powdered crystalline materials which had been heated to 280 °C in the DSC pan and halted the heating prior to melting. We measured their powder diffraction spectra and identified polymorph **H_3** in each case.

Conclusions

The polymorphs of the diol host compound show strong structural similarities as depicted by their Hirshfeld surface fingerprint plots, which exhibit dominant H···H interactions. The conformation of the molecule remains essentially constant, and is governed by an intramolecular O–H···O hydrogen bond in the polymorphs of the apohost and in all the nine inclusion compounds analysed. A remarkable feature of the four clathrates (**H·3P**, **H·2P·M**, **H·2P·B** and **H·P·M·B**) is that they have a host : guest ratio of 1 : 3 but are isostructural irrespective of the nature of the guest. The stoichiometries of these compounds can be controlled by the temperature of crystallization and their thermal decomposition can be correlated with their structures.

Experimental

Polymorphs of the apohost were crystallised at 25 °C from methanol (**H_1**), and **H_2** and **H_3** crystallised concomitantly from a mixture of acetone and 2-butanol in equimolar ratios.

The inclusion compounds were crystallised by slow evaporation or slow cooling from the following solvents at the specific temperatures:

H·3P from pure pyridine at 25 °C.

H·2P·M from an equimolar mixture of pyridine and morpholine at 25 °C.

H·2P·B from an equimolar mixture of pyridine and benzene at 25 °C

H·P·M·B from an equimolar mixture of pyridine, morpholine and benzene at 25 °C.

H·M and **H·3M** concomitantly from pure morpholine cooled from 25 °C to 0 °C, with **H·3M** predominating at the lower temperatures.

H·2P·3M from an equimolar mixture of pyridine and morpholine cooled to −20 °C.

H·2M·0.5B and **H·M·1.5B** from equimolar mixtures of morpholine and benzene at 25 °C and −20 °C, respectively.

The X-ray intensity data were collected on a Nonius Kappa CCD diffractometer using graphite-monochromated Mo-Kα radiation (λ = 0.71069 Å) with the crystal cooled to 113 ± 1 K by a Cryostream cooler (Oxford Cryostream, UK). The strategies of a combination of ϕ- and ω-scans for the data collection were evaluated using the COLLECT software.[21] Unit cell refinement and data reduction were performed with the program DENZO-SMN.[22] All the structures were solved by direct methods and refined by full-matrix least squares on F^2 using the program SHELX-97.[23] Programs were run using the graphic interface X-SEED.[24] Unless otherwise specified in the structural results and discussion, the following routine procedures were applied: All non-H atoms were refined anisotropically and hydrogens involved in hydrogen bonding were located by difference Fourier methods and the remaining hydrogens were included in idealised positions in a riding model with U_{iso} set at 1.2 or 1.5 times those of the parent atoms.

X-Ray powder diffraction (XPRD) patters were recorded with Cu-Kα radiation (λ = 1.5418 Å) on a Philip PW 1050/80 vertical goniometer equipped with a PW3710 control unit. Step scans of 0.1° and 20 s counts were employed in the 2θ range 6–40°. The theoretical XPRD patterns were computed with the program Lazy Pulverix[25] which uses the formula

$$I(hkl) = mLp|F(hkl)|^2,$$

where $I(hkl)$ is the intensity of the reflection with indices hkl, m is the reflection multiplicity, L the Lorentz factor, p the polarization factor, and $F(hkl)$ the structure factor.

Thermogravimetry (TGA) and differential scanning calorimetry (DSC) were performed on a Perkin-Elmer PC7 Series thermal station. TGA and DSC scans were recorded at 10 °C min^{-1} in the temperature range 30–340 °C with

sample masses in the range 2–5 mg. A nitrogen purge at 40 mL min^{-1} was used for both techniques.

Acknowledgements

We thank Professor Mark Spackman for his help in the analysis of the Hirshfeld surface fingerprint plots.

References

1 E. Weber, in *Inclusion Compounds*, ed. J. L. Atwood, J. E. D. Davies and D. D. MacNicol, Oxford University Press, Oxford, 1991, vol. 4, p. 188.
2 M. R. Caira, A. Horne, L. R. Nassimbeni and F. Toda, *J. Mater. Chem.*, 1997, **7**, 2145.
3 D. R. Bond, L. Johnson, L. R. Nassimbeni and F. Toda, *J. Solid State Chem.*, 1991, **92**, 68.
4 M. R. Caira, T. Le Roex, L. R. Nassimbeni, J. A. Ripmeester and E. Weber, *Org. Biomol. Chem.*, 2004, 2299.
5 E. Weber, in *Compreshensive Supramolecular Chemsitry*, ed. D. D. MacNicol, F. Toda and R. Bishop, Pergamon, Oxford, 1996, vol. 6, ch. 17.
6 M. R. Caira, A. Jacobs, L. R. Nassimbeni and F. Toda, *J. Chem. Crystallogr.*, 2006, **36**, 435.
7 M. R. Caira, L. R. Nassimbeni, F. Toda and D. Vujovic, *J. Chem. Soc., Perkin Trans. 2*, 2001, 2119.
8 M. R. Caira, L. R. Nassimbeni, F. Toda and D. Vujovic, *J. Am. Chem. Soc.*, 2000, **122**, 9367.
9 A. Bacchi, E. Bosetti, M. Carcelli, P. Pelagatti, D. Rogolino and G. Pelizzi, *Inorg. Chem.*, 2005, **44**, 431.
10 A. Bacchi, E. Bosetti and M. Carcelli, *CrystEngComm*, 2005, **7**, 527.
11 E. Weber and M. Czugler, Molecular Inclusion and Molecular Recognition-Clathrates II, *Top. Curr. Chem.*, 1988, **149**, 45.
12 E. Weber, K. Skobridis, A. Wierig, L. J. Barbour, M. R. Caira and L. R. Nassimbeni, *Chem. Ber.*, 1993, **126**, 1141.
13 A. L. Spek, *Acta Crystallogr., Sect. A*, 1990, **46**, C34.
14 J. J. McKinnon, M. A. Spackman and A. S. Mitchell, *Acta Crystallogr., Sect. B*, 2004, **60**, 627.
15 M. A. Spackman and J. J. McKinnon, *CrystEngComm*, 2002, **4**, 378.
16 S. K. Wolff, D. J. Grimwood, J. J. McKinnon, D. Jayatilaka and M. A. Spackman, *CrystalExplorer 2.0*, University of Western Australia, Perth, Australia.
17 M. R. Caira, A. Coetzee, K. R. Koch, L. R. Nassimbeni and F. Toda, *J. Chem. Soc., Perkin Trans. 2*, 1996, 569.
18 L. J. Barbour, S. A. Bourne, M. R. Caira, L. R. Nassimbeni, E. Weber, K. Skobridis and A. Wierig, *Supramol. Chem.*, 1993, **1**, 331.
19 E. Weber, K. Skobridis, A. Wierig, S. Stathi, L. R. Nassimbeni and M. Niveu, *Angew. Chem., Int. Ed. Engl.*, 1993, **32**, 606.
20 K. Skobridis, V. Theodorou, D. Alivertis, W. Seichter, E. Weber and I. Csoregh, *Supramol. Chem.*, 2007, **19**, 373.
21 COLLECT data collection software: Nonius BV, Delft, The Netherlands, 2000.
22 Z. Otwinowski and W. Minor, *Methods Enzymol.*, 1997, **276**, 307.
23 G. M. Sheldrick, *SHELXL-97: Program for the Refinement of Crystal Structures*, University of Göttingen, 1997.
24 L. J. Barbour, X-Seed: A Software Tool for Supramolecular Crystallography, *J. Supramol. Chem.*, 2001, **1**, 189.
25 K. Yvon, W. Jeitschko and E. Parthe, *J. Appl. Crystallogr.*, 1977, **10**, 73.